Novel coronavirus disease 2019 (COVID-19): relationship between chest CT scores and laboratory parameters

Bin Zhang[1] · Jue Zhang[2] · Hui Chen[3] · Luyan Chen[1] · Qiuying Chen[1] · Minmin Li[1] · Zhuozhi Chen[1] · Jingjing You[1] · Ke Yang[2] · Shuixing Zhang[1] 🔟

Abstract

Purpose To quantify the severity of 2019 novel coronavirus disease (COVID-19) on chest CT and to determine its relationship with laboratory parameters.

Methods Patients with real-time fluorescence polymerase chain reaction (RT-PCR)–confirmed COVID-19 between January 01 and February 18, 2020, were included in this study. Laboratory parameters were retrospectively collected from medical records. Severity of lung changes on chest CT of early, progressive, peak, and absorption stages was scored according to the percentage of lung involvement (5 lobes, scores 1–5 for each lobe, range 0–20). Relationship between CT scores and laboratory parameters was evaluated by the Spearman rank correlation. The Bonferroni correction adjusted significance level was at $0.05/4 = 0.0125$.

Results A total of 84 patients (mean age, 47.8 ± 12.0 years [standard deviation]; age range, 24–80 years) were evaluated. The patients underwent a total of 339 chest CT scans with a median interval of 4 days (interquartile range, 3–5 days). Median chest CT scores peaked at 4 days after the beginning of treatment and then declined. CT score of the early stage was correlated with neutrophil count ($r = 0.531$, $P = 0.011$). CT score of the progressive stage was correlated with neutrophil count ($r = 0.502$, $P < 0.001$), white blood cell count ($r = 0.414$, $P = 0.001$), C-reactive protein ($r = 0.511$, $P < 0.001$), procalcitonin ($r = 0.423$, $P = 0.004$), and lactose dehydrogenase ($r = 0.369$, $P = 0.010$). However, CT scores of the peak and absorption stages were not correlated with any parameter ($P > 0.0125$). No sex difference occurred regarding CT score ($P > 0.05$).

Conclusion Severity of lung abnormalities quantified on chest CT might correlate with laboratory parameters in the early and progressive stages. However, larger cohort studies are necessary.

Keywords COVID-19 · Chest CT · Laboratory parameters

Bin Zhang and Jue Zhang contributed equally to this work.

This article is part of the Topical Collection on Infection and Inflammation

✉ Ke Yang
tmyangke2019@sina.com

✉ Shuixing Zhang
shui7515@126.com

1 Department of Radiology, The First Affiliated Hospital of Jinan University, No. 613 Huangpu West Road, Tianhe District, Guangzhou 510627, Guangdong, China

2 Department of Radiology, The First People's Hospital of Tianmen City, No.1 Jingling Renmin East Road, Tianmen City 431700, Hubei Province, China

3 Department of Oncology, The First People's Hospital of Tianmen City, Tianmen, Hubei, China

Introduction

Novel coronavirus disease 2019 (COVID-19) was first reported in Wuhan, Hubei province, and rapidly spread to other provinces/regions of China and other countries [1]. At the time of writing this article, COVID-19 has affected 74,680 people. The epidemiological, clinical, laboratory, and radiologic (thin-section computed tomography [CT]) characteristics have been published recently [2–5]. The radiographic features at presentation included peripheral and bilateral ground-glass opacities (GGO), which progressed with consolidation in most of COVID-19 patients [6–9].

The alanine aminotransferase (ALT) and aspartate aminotransferase (AST) levels were reportedly increasing 23–100% and 70–78% in severe acute respiratory syndrome (SARS) patients, respectively [10–14]. A recent study took biopsy samples from the lung, liver, and heart tissue of a patient

who died of COVID-19 [15]. The pathological findings of the lung showed bilateral diffuse alveolar damage with cellular fibromyxoid exudates and interstitial mononuclear inflammatory infiltrates (mainly lymphocytes). The biopsy specimens of the liver showed moderate microvascular steatosis and mild lobular and portal activity, suggesting the injury maybe induced by novel coronavirus or drugs. No obvious histological changes were seen in the heart specimens, suggesting coronavirus infection may not directly damage the heart. Although we already knew the pathological changes of multiple organs in a critically ill patient with COVID-19, little is known about the potential association between the temporal dynamic changes of the lung and other organs. The aim of this study, therefore, was to quantify the severity of lung involvement on chest CT and to determine the relationship between lung severity and laboratory parameters of infection and organ function in different disease stages, which might benefit patient care.

Materials and methods

The retrospective study was approved by the ethics committee of the First Affiliated Hospital of Jinan University, with a waiver of informed consent. From January 01 to February 18, 2020, a total of 103 COVID-19 patients were admitted to The First People's Hospital of Tianmen City, Hubei Province. All the patients were positive for COVID-19 via real-time fluorescence polymerase chain reaction (RT-PCR) for COVID-19 nucleic acid by bronchoalveolar lavage, endotracheal aspirate, nasopharyngeal swab, or oropharyngeal swab. Critically ill patients ($n = 13$) and patients with consistently normal chest CT ($n = 6$) were excluded. Critically ill patients were defined as having one of the following conditions [16]: (1) respiratory failure occurs and requires mechanical ventilation; (2) septic shock; (3) complicated with other organ failures requiring intensive care unit management. The patients underwent chest CT by a CT 64 scanner (GE Medical System), Siemens Emotion 16 scanner (Siemens Healthineers; Erlangen, Germany), and ICT 128 scanner (Philips Healthcare, Netherlands), with images indicating a 1- or 1.25-mm slice thickness. We obtained patients' laboratory parameters from medical records, including lymphocyte count (normal range, $1.1–3.2 \times 10^9$/L), neutrophil count (normal range, $1.8–6.3 \times 10^9$/L), white blood cell (WBC) count (normal range, $3.5–9.5 \times 10^9$/L), hemoglobin (normal range, 130–175 g/L), platelet count ($125–350 \times 10^9$/L), C-reactive protein (CRP) (normal range, $\leq$ 6 mg/L), procalcitonin (normal range, 0–0.046 ng/mL), lactose dehydrogenase (LDH) (normal range, 120–250 U/L), alanine aminotransferase (ALT) (normal range, 7–40 U/L), aspartate aminotransferase (AST) (normal range, 13–35 U/L), creatine kinase (CK) (normal range, 40–200 U/L),

creatine kinase isoenzyme (CK-MB) (normal range, 0–24 U/L), activated partial thromboplastin time (APTT) (normal range, 22–38 s), prothrombin time (PT) (normal range, 10–14 s), and creatinine (normal range, 57–111 μmol/L). All the patients received antiviral drugs (e.g., oseltamivir, arbidol, interferon, Yanhuning, or kaletra) and anti-inflammatory drugs (e.g., moxifloxacin and/or cefoperazone sodium and tazobactam), and most severe patients received methylprednisolone. All the patients were followed up by chest CT, which could be classified into four stages: early, progressive, peak, and absorption stages [17]. The dates of chest CT and laboratory examination were well-matched. An overall lung total severity score (CT score) (range 0–20 points) was assigned according to Chung et al. [6]. All chest CT images were reviewed independently by two cardiothoracic radiologists with more than 10 years of experience. Final decisions were reached by consensus.

Statistical analysis

All chest CT scores were correlated with laboratory parameters at days of early, progressive, peak, and absorption stages using the Spearman rank correlation. The Bonferroni correction adjusted significance level was $0.05/4 = 0.0125$. Sex difference with respect to laboratory and radiological parameters was also evaluated by the Mann-Whitney U test. Difference between laboratory and radiographic data was obtained at early, progressive, peak, and absorption stages using one-way analysis of variance (ANOVA) with post hoc Tukey's multiple comparison tests at a level of significance $P < 0.05$. The peak stage was used as the reference stage.

Results

Clinical characteristics

The mean age of the 84 patients was 47.8 ± 12.0 years (median age, 49.0 years; age range, 24–80 years). There were 50 (60%) male and 34 (40%) female patients. The mean age for male was 49.3 ± 12.9 years (median age, 50.5 years; age range, 24–80 years) and that for female was 45.4 ± 10.3 years (median age, 47.5 years; age range, 24–67 years), with no significant difference ($P = 0.142$). A total of 339 chest CT scans (including 5 normal scans at admission) were performed and each patient underwent a median of 4 CT scans (interquartile range, 3–5) with a median interval of 4 days (interquartile range, 3–5 days). Specifically, 69 chest CT scans, 157 chest CT scans, 25 chest CT scans, and 83 chest CT scans were performed for early, progressive, peak, and absorption stages, respectively. Table 1 summarizes the radiologic and laboratory parameters for the 84 patients. CT score, WBC count, and

Table 1 Radiological and laboratory parameters in 84 patients

Parameter	Early stage ($n = 69$)	Progressive stage ($n = 157$)	Peak stage ($n = 25$)	Absorption stage ($n = 83$)	P value[#]
CT score	$4.79 \pm 2.00^{++}$	$7.88 \pm 3.00^{++}$	13.10 ± 2.13	$7.07 \pm 2.84^{++}$	< 0.001**
	5.00, 1.00–10.00	8.00, 2.00–13.00	13.00, 10.00–18.00	7.00, 1.00–13.00	
Lymphocyte count, $\times 10^9$/L	1.38 ± 0.56	1.26 ± 0.44	1.03 ± 0.56	$1.48 \pm 0.49^{+}$	0.046*
	1.25, 0.78–2.95	1.18, 0.56–2.44	1.01, 0.38–1.70	1.47, 0.40–2.63	
Neutrophil count, $\times 10^9$/L	$2.84 \pm 1.32^{+}$	3.64 ± 2.21	5.01 ± 2.84	3.94 ± 1.92	0.028*
	2.43, 0.91–6.77	3.09, 1.15–13.52	4.74, 1.74–9.81	3.50, 1.82–10.15	
WBC count, $\times 10^9$/L	$4.76 \pm 1.48^{+}$	5.44 ± 2.25	6.66 ± 2.95	6.06 ± 1.85	0.081
	4.36, 2.72–8.86	5.19, 2.70–14.67	6.76, 3.11–10.49	5.44, 3.11–12.18	
Hemoglobin, g/L	132.26 ± 21.85	126.05 ± 23.16	131.00 ± 24.58	127.67 ± 13.39	0.626
	135.50, 74.00–172.00	130.00, 13.10–162.00	133.50, 77.00–161.00	126.00, 102.00–155.00	
Platelet count, $\times 10^9$/L	$189.12 \pm 84.51^{++}$	$227.54 \pm 91.38^{+}$	331.80 ± 113.50	267.31 ± 67.39	0.001*
	173.00, 81.00–566.00	215.00, 55.00–543.00	325.00, 173.00–533.00	264.50, 51.00–445.00	
CRP, mg/L	31.92 ± 35.90	35.47 ± 38.44	23.11 ± 29.80	4.46 ± 12.67	0.859
	13.43, 0.50–136.09	21.30, 0.50–150.32	13.02, 1.31–100.35	1.17, 0.50–80.09	
Procalcitonin, ng/mL	0.04 ± 0.03	0.05 ± 0.04	0.04 ± 0.02	0.07 ± 0.08	0.579
	0.04, 0.02–0.10	0.04, 0.02–0.23	0.04, 0.02–0.06	0.04, 0.02–0.27	
AST, U/L	29.09 ± 13.71	29.74 ± 20.38	26.09 ± 10.87	21.66 ± 9.70	0.822
	27.05, 11.50–79.20	22.30, 8.50–104.30	23.60, 14.10–42.40	18.00, 10.00–56.10	
ALT, U/L	34.40 ± 28.98	36.07 ± 44.36	55.51 ± 34.38	38.55 ± 30.07	0.139
	27.30, 8.80–138.30	21.70, 7.10–221.60	49.10, 15.60–110.20	24.30, 10.20–135.80	
LDH, U/L	242.08 ± 107.28	263.15 ± 83.42	285.00 ± 34.98	184.75 ± 22.58	0.271
	218.00, 149.00–669.00	230.00, 151.00–500.00	288.00, 226.00–336.00	185.50, 151.00–219.00	
CK, U/L	140.69 ± 173.47	$73.54 \pm 60.61^{+}$	353.71 ± 770.51	45.00 ± 23.98	0.004*
	71.00, 33.00–715.00	59.00, 18.00–384.00	71.00, 28.00–2100.00	39.50, 19.00–89.00	
CK-MB, U/L	11.08 ± 4.81	10.00 ± 5.45	13.20 ± 10.73	9.38 ± 2.93	0.169
	9.82, 5.51–26.37	9.02, 1.75–32.10	7.97, 5.06–32.55	9.18, 4.25–14.93	
APTT, s	30.00 ± 4.56	30.77 ± 6.88	25.18 ± 6.69	26.17 ± 4.10	0.059
	29.80, 23.10–42.10	30.30, 16.60–57.70	24.65, 17.60–33.90	24.35, 23.70–32.30	
PT, s	12.42 ± 0.71	12.28 ± 0.70	12.48 ± 0.50	11.62 ± 0.74	0.483
	12.30, 11.00–14.80	12.10, 11.20–14.50	12.55, 11.70–13.10	11.55, 10.80–12.60	
Creatinine, μmol/L	72.44 ± 20.34	71.04 ± 21.29	67.90 ± 18.40	65.14 ± 16.95	0.822
	69.55, 37.90–113.40	63.65, 41.20–140.00	70.50, 41.30–99.90	63.45, 27.10–104.80	

Values are the mean ± SD or median and interquartile range

[#] One-way ANOVA analysis with post hoc tests was used to test the differences between data at the early, progressive, peak, and absorption stages

[+] $P < 0.05$, comparison between data at the early, progressive, absorption, and peak stages

[++] $P < 0.001$, comparison between data at the early, progressive, absorption, and peak stages

*$P < 0.05$

**$P < 0.001$

CT computed tomography; *WBC* white blood cell; *CRP* C-reactive protein; *LDH* lactose dehydrogenase; *ALT* alanine aminotransferase; *AST* aspartate aminotransferase; *CK* creatine kinase; *CK-MB* creatine kinase isoenzyme; *APTT* activated partial thromboplastin time; *PT* prothrombin time

neutrophil count were significantly higher in the peak stage as compared with those obtained at the early stage ($P < 0.001$), progressive stage ($P < 0.001$), and absorption stage ($P < 0.001$). At the end of February 18, 2020, only 1 (1.2%) patient died of the disease, 44 (52.4%) remained in the hospital, and 39 (46.4%) were discharged from the hospital.

Imaging features

The major CT findings were compared at early, progressive, peak, and absorption stages (Table 2). In the early stage, the most frequent CT appearance was bilateral GGO with peripheral distribution (Fig. 1a). In addition, consolidation, crazy-paving pattern, bronchiectasis, and reverse halo sign could

Table 2 Imaging features of lung lesions on chest CT in different stages

	Early stage (n = 69)	Progressive stage (n = 157)	Peak stage (n = 25)	Absorption stage (n = 83)
Involvement of the lesions				
Single lobe	12 (17.4)	3 (1.9)	0	2 (2.4)
Two lobes	10 (14.5)	10 (6.4)	0	4 (4.8)
Three lobes	12 (17.4)	14 (8.9)	0	14 (16.9)
Four lobes	12 (17.4)	15 (9.6)	0	6 (7.2)
Five lobes	23 (33.3)	115 (73.2)	25 (100)	57 (68.7)
GGO				
None	0	4 (2.5)	0	2 (2.4)
Yes	69 (100)	153 (97.5)	25 (100)	81 (97.6)
Crazy-paving pattern				
None	42 (60.9)	103 (65.6)	11 (44)	77 (92.8)
Yes	27 (39.1)	54 (34.4)	14 (56)	6 (7.2)
Consolidation				
None	47 (68.1)	18 (11.5)	0	39 (47.0)
Yes	22 (31.9)	139 (88.5)	25 (100)	44 (53.0)
Pulmonary fibrosis				
None	69 (100)	105 (66.9)	16 (64)	29 (34.9)
Yes	0	52 (33.1)	9 (36)	54 (65.1)
Bronchiectasis				
None	37 (53.6)	63 (40.1)	7 (28)	70 (84.3)
Yes	32 (46.4)	94 (59.9)	18 (72)	13 (15.7)
Pleural effusion				
None	69 (100)	154 (98.1)	23 (92)	82 (98.8)
Yes	0	3 (1.9)	2 (8)	1 (1.2)
Cavitation				
None	69 (100)	155 (98.7)	25 (100)	83 (100)
Yes	0	2 (1.3)	0	0
Reverse halo sign				
None	68 (98.6)	157 (100)	25 (100)	83 (100)
Yes	1 (1.4)	0	0	0

Numbers in parentheses are percentages

be found in some patients. In the progressive stage, extensive GGO with consolidation, crazy-paving pattern, and traction bronchiectasis was often observed (Fig. 1b). In a small proportion of cases, pleural effusion and cavitation could be seen. In the peak stage, the diffuse GGO further extended to peak, with consolidation becoming denser (Fig. 1c). In the absorption stage, the consolidation was gradually absorbed with residual parenchymal bands (Fig. 1d). Few cases presented crazy-paving pattern. Figure 2 shows the progression pattern or stage of the disease as of February 18, 2020. At admission, 5 (6.0%) patients' chest CT scans were normal, 51 (60.7%) were at early stage, and 28 (33.3%) were at progressive stage. Early-progressive-absorption stage was the most frequent (34.5%) pattern. Only 11 (13%) patients experienced peak stage of the disease.

Relationship between the CT scores and laboratory parameters

The mean CT scores of the early, progressive, peak, and absorption stages were 4.8 ± 2.0, 7.1 ± 2.8, 13.1 ± 2.1, and 7.1 ± 2.8, respectively, with significant difference among the four stages ($P < 0.001$). Median chest CT scores peaked at 4 days after the beginning of treatment and then declined.

The early stage CT score was correlated with neutrophil count ($r = 0.531$, $P = 0.011$). The progressive stage CT score was correlated with neutrophil count ($r = 0.502$, $P < 0.001$), WBC count ($r = 0.414$, $P = 0.001$), CRP ($r = 0.511$, $P < 0.001$), procalcitonin ($r = 0.423$, $P = 0.004$), and LDH ($r = 0.369$, $P = 0.010$). However, there were no relationship

Fig. 1 Typical evolution of CT findings in a 46-year-old female presenting with fever for 4 days. **a** Axial chest CT obtained at presentation shows subpleural ground-glass opacities (GGO) in the right upper and lower lobes. **b** Axial chest CT obtained at day 5 of treatment shows enlarged region of GGO with interlobular septal thickening (crazy-paving pattern) and partial consolidation. **c** Axial chest CT obtained at day 9 of treatment shows increased consolidation. **d** Axial chest CT obtained at day 13 shows significant absorption of consolidation with residual parenchymal bands
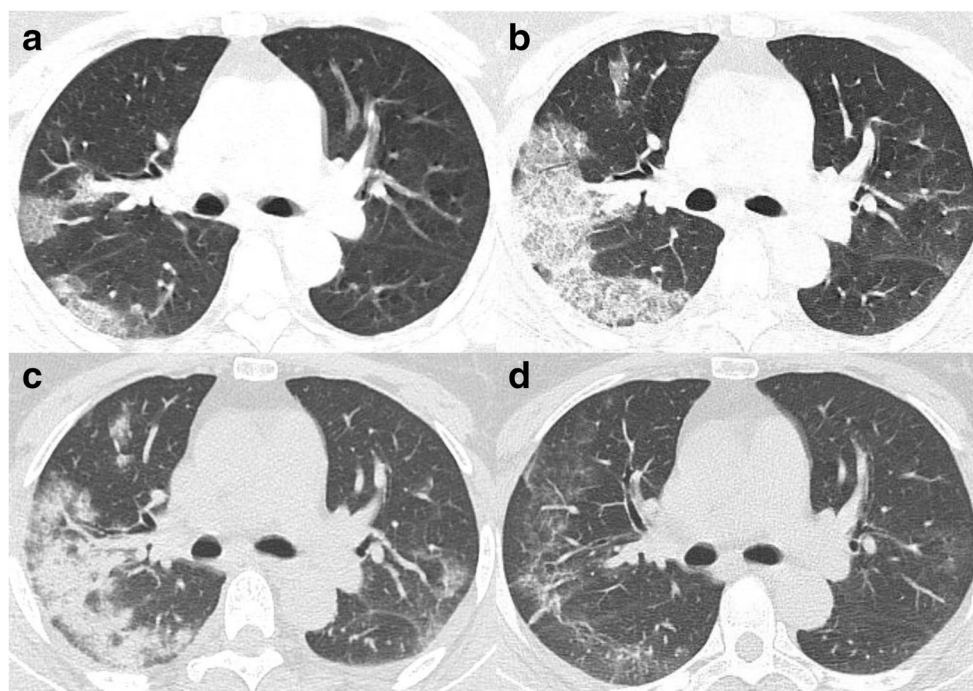
between CT scores of peak and absorption stages and all laboratory parameters ($P > 0.0125$).

While patients were stratified according to sex, there was no significant difference with respect to CT score ($P > 0.05$). Significant difference was observed in CRP ($P = 0.010$ in the early stage), CK ($P = 0.007$ in the early stage), AST ($P = 0.005$ in the early stage), neutrophil count ($P = 0.046$ in the absorption stage), platelet count ($P = 0.034$ in the absorption stage), WBC count ($P = 0.016$ in the progressive stage and 0.041 in the absorption stage), procalcitonin ($P = 0.003$ in the progressive stage), ALT ($P < 0.05$ in the early, progressive, and absorption stages), hemoglobin ($P < 0.001$ in all stages), and creatinine ($P \leq 0.001$ in all stages).

Discussion

The findings of this clinical and radiological study in a cohort of patients with COVID-19 infection showed that the severity of lung abnormalities quantified on chest CT was positively correlated with laboratory parameters in the early and progressive stages. CT scores peaked at about 4 days after the beginning of treatment and then declined, which generally reflected temporal changes in laboratory parameters after the start of treatment. In the absence of more specific disease biomarkers, chest CT, therefore, appears to be a useful and effective tool for patient assessment.

In the early stage, the relationship between neutrophil count and CT score indicated the early inflammatory response

Fig. 2 The progression pattern or stage of COVID-19 on chest CT as of February 18, 2020
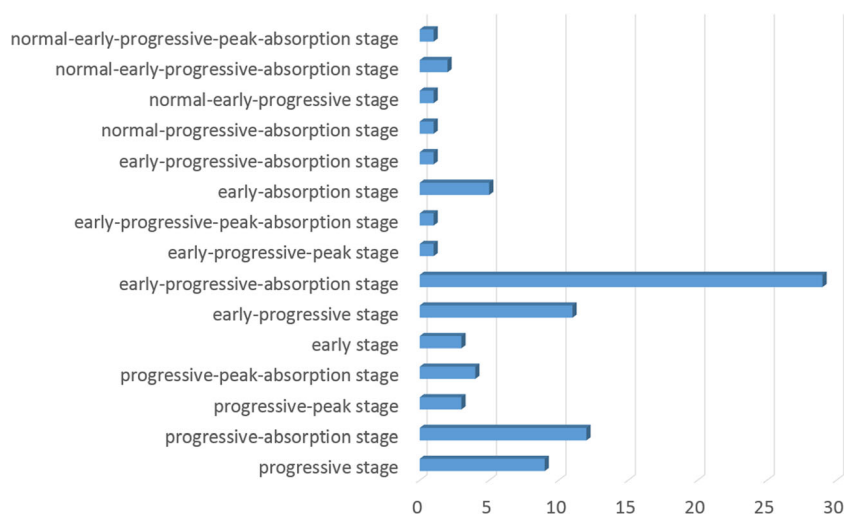
caused by pneumonias. Neutrophilia is one of the hallmarks of acute infection. Neutrophils are recruited early to sites of infection where they kill pathogens (bacteria, fungi, and viruses) by oxidative burst and phagocytosis [18]. Some literature supported the hypothesis that a little known yet powerful function of neutrophils—the ability to form neutrophil extracellular traps—may contribute to organ damage and death in COVID-19 [19]. Previous studies showed neutrophil count was notably related to disease severity [20, 21]. Neutrophil infiltration was noted in two recent reports on the pathological findings from autopsied COVID-19 patients [22, 23]. In the progressive stage, infection-related biomarkers included neutrophil count, WBC, CRP, and procalcitonin elevated. Pathological findings showed diffuse alveolar damage with inflammatory cell infiltration in this stage. Accordingly, chest CT showed diffuse GGO with consolidation. Patients with severe virus infection are more likely to be co-infected with bacteria due to low immune functions [24]. Cytokine storm in severe and critically ill patients with COVID-19 might be associated with the activity of these infection-related biomarkers regulated by inflammatory cytokine.

In the peak stage, we found no linkage between CT scores and laboratory parameters, which might be due to the treatment effect of antiviral and antibacterial drugs as well as the small sample size. The changes of CT images might lag behind the changes of laboratory parameters. In the absorption stage, the laboratory parameters did not correlate with CT scores, which might be due to the mismatch between CT scores and inflammatory clearance. The CT scores in the absorption stage were not significantly reduced compared with those in progressive stage because consolidation generally dissipated into GGO and extensive GGO was noted after consolidation absorption. Another explanation might be the changes of chest CT lagged behind the changes of laboratory indexes.

The limitations of this study should be acknowledged. Firstly, this was a retrospective study and the sample size was relatively small, especially for the peak stage. Secondly, there was a selection bias due to the exclusion of critically ill patients. Hence, the findings of this study could only be applied to patients with moderate and severe COVID-19.

In conclusion, the results of this study indicated that disease severity on chest CT peaked at about 4 days after the beginning of treatment, followed by a general decline. Our findings showed the severity of abnormalities quantified on the chest CT might positively correlate with laboratory parameters in the early and progressive stages. However, larger cohort studies are needed to confirm these findings. This study might provide an insight into the appropriate follow-up interval of chest CT to reduce radiation and also indicate the indispensable role of chest CT in monitoring disease progression and therapeutic effect.

Compliance with ethical standards

Conflict of interest The authors declare that they have no conflict of interest.

Ethical approval All procedures performed in this study involving human participants were in accordance with the ethical standards of the institutional and/or national research committee and with the 1964 Helsinki declaration and its later amendments or comparable ethical standards.

Informed consent Informed consent was waived by the ethics committee of our institutions.

References

1. Zhu N, Zhang D, Wang W, et al. A novel coronavirus from patients with pneumonia in China, 2019. N Engl J Med. 2020;382:727–33.
2. Wang D, Hu B, Hu C, et al. Clinical characteristics of 138 hospitalized patients with 2019 novel coronavirus-infected pneumonia in Wuhan, China. JAMA. 2020. https://doi.org/10.1001/jama.2020.1585.
3. Chen N, Zhou M, Dong X, et al. Epidemiological and clinical characteristics of 99 cases of 2019 novel coronavirus pneumonia in Wuhan, China: a descriptive study. Lancet. 2020;395:507–13.
4. Chang D, Lin M, Wei L, et al. Epidemiologic and clinical characteristics of novel coronavirus infections involving 13 patients outside Wuhan, China. JAMA. 2020. https://doi.org/10.1001/jama.2020.1623.
5. Xu XW, Wu XX, Jiang XG, et al. Clinical findings in a group of patients infected with the 2019 novel coronavirus (SARS-Cov-2) outside of Wuhan, China: retrospective case series. BMJ. 2020;368:m606.
6. Chung M, Adam B, Mei X, et al. CT Imaging Features of 2019 Novel coronavirus (2019-nCoV). Radiology. 2020. https://doi.org/10.1148/radiol.2020200230.
7. Song F, Shi N, Shan F, et al. Emerging coronavirus 2019-nCoV pneumonia. Radiology. 2020;295:210–7.
8. Fang Y, Zhang H, Xu Y, et al. CT manifestations of two cases of 2019 novel coronavirus (2019-nCoV) pneumonia. Radiology. 2020. https://doi.org/10.1148/radiol.2020200280.
9. Shi H, Han X, Zheng C. Evolution of CT manifestations in a patient recovered from 2019 novel coronavirus (2019-nCoV) pneumonia in Wuhan, China. Radiology. 2020;295:20.
10. Lee N, Hui D, Wu A, et al. A major outbreak of severe acute respiratory syndrome in Hong Kong. N Engl J Med. 2003;348:1986–94.
11. Poutanen SM, Low DE, Henry B, et al. Identification of severe acute respiratory syndrome in Canada. N Engl J Med. 2003;348:1995–2005.

12. Hsu LY, Lee CC, Green JA, et al. Severe acute respiratory syndrome (SARS) in Singapore: clinical features of index patient and initial contacts. Emerg Infect Dis. 2003;9:713–7.

13. Peiris JSM, Lai ST, Poon LLM, et al. Coronavirus as a possible cause of severe acute respiratory syndrome. Lancet. 2003;361:1319–25.

14. Tsang KW, Ho PL, Ooi GC, et al. A cluster of cases of severe acute respiratory syndrome in Hong Kong. N Engl J Med. 2003;348:1977–85.

15. Xu Z, Shi L, Wang Y, et al. Pathological findings of COVID-19 associated with acute respiratory distress syndrome. Lancet Respir Med. 2020;8:420–2.

16. National Health Commission of the People's Republic of China. Guidelines for the diagnosis and treatment of novel coronavirus (2019-nCoV) infection (trial version 5) (in Chinese). 2020. https://doi.org/10.7661/j.cjim.20200202.064.

17. Feng P, Tianhe Y, Peng S, et al. Time course of lung changes on chest CT during recovery from 2019 novel coronavirus (COVID-19) pneumonia. Radiology. Published Online: Feb 13 2020. https://doi.org/10.1148/radiol.2020200370.

18. Schönrich G, Raftery MJ. Neutrophil extracellular traps go viral. Front Immunol. 2016;7:366.

19. Barnes BJ, Adrover JM, Baxter-Stoltzfus A, et al. Targeting potential drivers of COVID-19: neutrophil extracellular traps. J Exp Med. 2020;217(6). https://doi.org/10.1084/jem.20200652.

20. Zhang G, Zhang J, Wang B, et al. Analysis of clinical characteristics and laboratory findings of 95 cases of 2019 novel coronavirus pneumonia in Wuhan, China: a retrospective analysis. Respir Res. 2020;21:74.

21. Mo P, Xing Y, Xiao Y, et al. Clinical characteristics of refractory COVID-19 pneumonia in Wuhan, China. Clin Infect Dis. 2020. https://doi.org/10.1093/cid/ciaa270.

22. Yao XH, Li TY, He ZC, et al. A pathological report of three COVID-19 cases by minimally invasive autopsies. Zhonghua Bing Li Xue Za Zhi. 2020;49:E009. https://sci-hub.tw/https://doi.org/10.3760/cma.j.cn112151-20200312-00193. Accessed 19 Feb 2020.

23. Fox SE, Akmatbekov A, Harbert JL, et al. Pulmonary and cardiac pathology in Covid-19: the first autopsy series from New Orleans. MedRxiv. https://sci-hub.tw/https://doi.org/10.1101/2020.04.06.20050575 (Preprint posted April 10, 2020).

24. Liu Y, Du X, Chen J, et al. Neutrophil-to-lymphocyte ratio as an independent risk factor for mortality in hospitalized patients with COVID-19. J Inf Secur. 2020. https://doi.org/10.1016/j.jinf.2020.04.002.